INTERNATIONAL JOURNAL FOR NUMERICAL METHODS IN FLUIDS
Int. J. Numer. Meth. Fluids 2000; **33**: 81–88

Control functions and grid qualities measurements in the elliptic grid generation around arbitrary surfaces

Sungcho Kim*

Department of Mechanical Engineering, College of Engineering, Sunchon National University, Sunchon, Chunnam, 540-742, South Korea

SUMMARY

This paper describes the three-dimensional elliptic grid generation. The two-dimensional approach for the control functions obtained by modifying the Thomas–Middlecoff method is applied on the planes perpendicular to the main flow direction co-ordinate, which is assumed to be the function of only one corresponding co-ordinate in the computational domain. The grid orthogonality is improved by about 40 per cent compared with that of the algebraic initial grid. Copyright © 2000 John Wiley & Sons, Ltd.

KEY WORDS: control functions; elliptic grid; grid qualities; transfinite interpolation

1. INTRODUCTION

The algebraic grid methods usually adopt transfinite interpolations combined with Bezier and B-spline curves to improve grid qualities. These techniques are usually good, however, they can not guarantee the orthogonality and the grid may be overlapped.

Since the grid size is actually restricted and the body surface shape should be considered, the most elliptic grids employ the adequate control functions to refine the grid. They resist grid line overlapping, are always smooth, and can be used for grid adaptation. The control point formulation using the polynomials is developed by Eiseman [1]. Thompson and Weatherill [2] and Thomas [3] evaluate the control functions on the boundaries by interpolation. Soni [4] presents cell area and grid spacing approaches to optimize the two-dimensional grid orthogonality. Soni [5] measures the grid qualities considering the truncation error caused by the non-uniform grid. Grid refinement can be pursued by the introduction of control functions found in the arc length parameter [6]. The grid qualities of a single block obtained for the complicated geometry may become poor, therefore multi-block or an unstructured grid system is alternatively recommended [7].

* Correspondence to: Department of Mechanical Engineering, College of Engineering, Sunchon National University (SNU), 315 Maegok-dong, Sunchon, Chunnam, 540-742, South Korea.

Received 31 August 1998
Revised 28 June 1999

In this paper, a three-dimensional elliptic structured grid system is easily generated with consideration of the control functions. The grid quality is also discussed.

2. GRID GENERATION

The body-fitted co-ordinates are generated by determining the curvilinear co-ordinates in the physical domain. This problem can be settled by solving the partial differential equation (PDE), and the extremum principles guarantee a one-to-one mapping between the physical and computational domains. The governing equations, obtained from both minimizing the integral of a grid point density and embedding the control functions, become Poisson-type systems, i.e.

$$\nabla^2 \xi^i = \phi^i, \quad i = 1, 2, 3 \tag{1}$$

where $\xi^i = (\xi, \eta, \zeta)$ is the computational space, $\boldsymbol{r} = (x, y, z)$ is the Cartesian co-ordinate, $\phi^i = (\phi, \psi, \theta) = g^{jk}\phi^i_{jk}$ $(j, k = 1, 2, 3)$ are the control functions, and g^{jk} are the contravariant metric tensors [8]. Equation (1) is transformed to be the quasi-linear elliptic PDE

$$\nabla^2 \boldsymbol{r} = g^{ij}(\boldsymbol{r}_{\xi^i \xi^j} + \phi^k_{ij}\boldsymbol{r}_{\xi^k}) = 0, \quad i, j, k = 1, 2, 3 \tag{2}$$

Equation (2) generates the grid system, and $\phi^i_{jk} = \delta^i_j \delta^i_k g^{ij}\phi_i$, where δ is the Kronecker delta. Eiseman [9] suggested algebraic techniques providing exact control of the mesh properties under the given constraints. Steger and Sorenson [10] introduced forcing functions to change intersection angles and spacings. In this paper, the control functions will be evaluated by solving the governing equations simultaneously, and the grid spacing is controlled in the nearest region of the body surface. Now Equation (2) can be rearranged as

$$g^{ij}\boldsymbol{r}_{\xi^i \xi^j} + g^{kk}\phi_k \boldsymbol{r}_{\xi^k} = 0, \quad i, j, k = 1, 2, 3 \tag{3}$$

In external flow calculations for ships, etc., $x = x(\xi)$ can be assumed [11] and thus Equation (3) reduces to a quasi-three-dimensional form, i.e.

$$\begin{bmatrix} g^{11}x_{\xi\xi} \\ q \\ p \end{bmatrix} = \begin{bmatrix} g^{11}\phi_1 \\ g^{22}\phi_2 \\ g^{33}\phi_3 \end{bmatrix}^T \begin{pmatrix} x_\xi & 0 & 0 \\ 0 & y_\eta & z_\eta \\ 0 & y_\zeta & z_\zeta \end{pmatrix} \tag{4a}$$

$$\begin{bmatrix} q \\ p \end{bmatrix} = \begin{bmatrix} g^{11} \\ g^{22} \\ g^{33} \end{bmatrix}^T \begin{pmatrix} y_{\xi\xi} - \phi_1 y_\xi & z_{\xi\xi} - \phi_1 y_\xi \\ y_{\eta\eta} & z_{\eta\eta} \\ y_{\zeta\zeta} & z_{\zeta\zeta} \end{pmatrix} + 2 \begin{bmatrix} g^{12} \\ g^{13} \\ g^{23} \end{bmatrix}^T \begin{pmatrix} y_{\xi\eta} & z_{\xi\eta} \\ y_{\xi\zeta} & z_{\xi\zeta} \\ y_{\eta\zeta} & z_{\eta\zeta} \end{pmatrix} \tag{4b}$$

Three control functions are easily determined as follows:

$$\begin{bmatrix} \phi_1 \\ g^{22}\phi_2 \\ g^{33}\phi_3 \end{bmatrix} = \frac{1}{A} \begin{bmatrix} \dfrac{Ax_{\xi\xi}}{x_\xi} & 0 & 0 \\ 0 & -y_\zeta & z_\zeta \\ 0 & -y_\eta & z_\eta \end{bmatrix} \begin{pmatrix} 1 \\ p \\ q \end{pmatrix} \tag{5}$$

where $A = y_\eta z_\zeta - z_\eta y_\zeta$. The three-dimensional distribution meshes are constructed by calculating the intersection of two adjacent lines on the projection plane.

Equation (3), with substituting the control functions, is finally expressed in the tri-diagonal system, where ξ is the main flow direction, and η is perpendicular to the body surface. Orthogonality is forced on the (y, z) plane, and the grid spacing is adjusted just near the body surface, i.e.

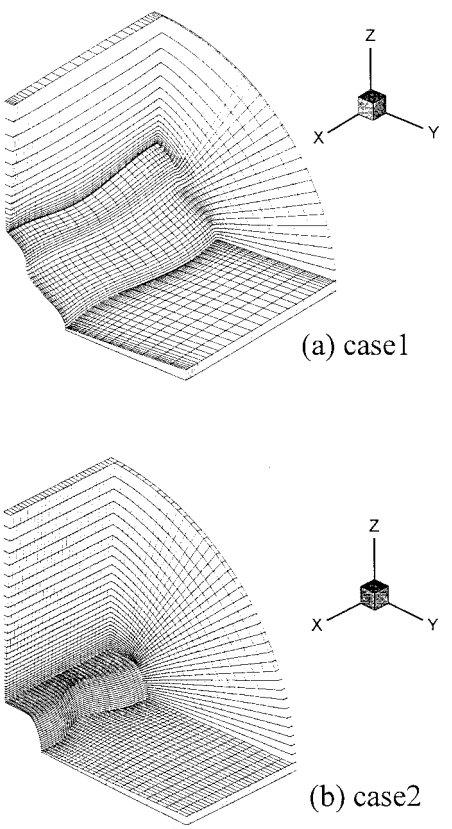

Figure 1. Test grid system.

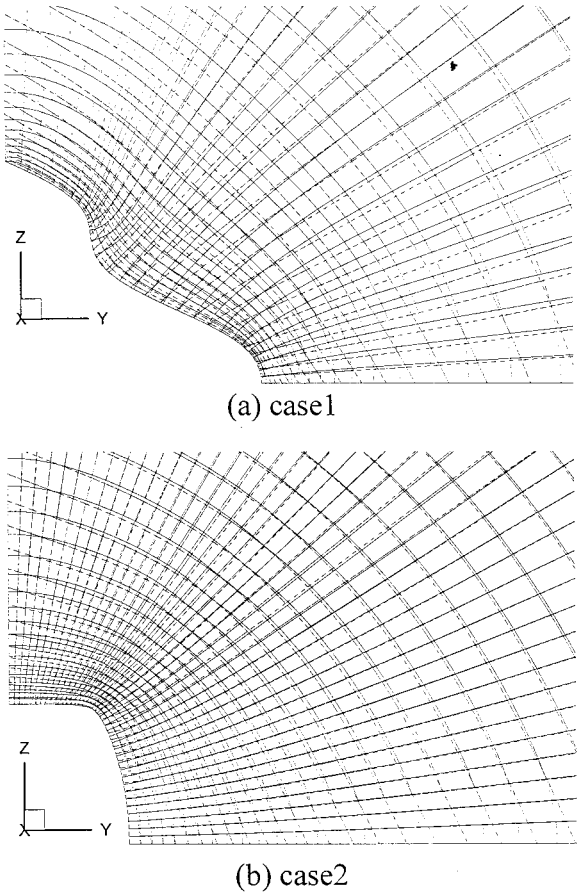

Figure 2. Comparison of the grids at the center position of x ($i = 15$) (solid, elliptic grid; dashed, algebraic grid).

$$\begin{bmatrix} y_\eta \\ z_\eta \end{bmatrix}^T \begin{pmatrix} y_\eta & y_\xi \\ y_\eta & z_\xi \end{pmatrix} = \begin{bmatrix} g_{22} \\ g_{23} \end{bmatrix} \tag{6}$$

where g_{ij} is the covariant metric tensor, $g_{23} = 0$ and $\sqrt{g_{22}}$ denote the chosen grid spaces just near the body surface. Then, two-dimensional analysis is applied in the (x, y) plane, where the control functions are chosen as Equation (7) by modifying the Thomas–Middlecoff method [12]

$$\begin{bmatrix} \phi_1 \\ \phi_2 \end{bmatrix} = \frac{1}{\sqrt{\Delta x^2 + \Delta y^2}} \begin{bmatrix} x_{\xi\xi} & y_{\xi\xi} \\ x_{\eta\eta} & y_{\eta\eta} \end{bmatrix} \begin{bmatrix} \Delta x \\ \Delta y \end{bmatrix} \tag{7}$$

The initial grid is generated linearly using three-dimensional transfinite interpolation (the Boolean form) as follows:

$$\boldsymbol{r}_\xi \oplus \boldsymbol{r}_\eta \oplus \boldsymbol{r}_\zeta = \boldsymbol{r}_\xi + \boldsymbol{r}_\eta + \boldsymbol{r}_\zeta - \boldsymbol{r}_\xi \boldsymbol{r}_\eta - \boldsymbol{r}_\eta \boldsymbol{r}_\zeta - \boldsymbol{r}_\xi \boldsymbol{r}_\zeta + \boldsymbol{r}_\xi \boldsymbol{r}_\eta \boldsymbol{r}_\zeta \tag{8}$$

This is a kind of univariate method and the terms in Equation (8) are derived as follows:

$$\boldsymbol{r}_\xi = \sum_{i=1}^{2} \alpha_i \boldsymbol{r}(\xi_i, \eta, \zeta), \qquad \boldsymbol{r}_\eta = \sum_{j=1}^{2} \beta_j \boldsymbol{r}(\xi, \eta_j, \zeta), \qquad \boldsymbol{r}_\zeta = \sum_{k=1}^{2} \gamma_k \boldsymbol{r}(\xi, \eta, \zeta_k)$$

$$\boldsymbol{r}_\xi \boldsymbol{r}_\eta = \sum_{i=1}^{2} \alpha_i \sum_{j=1}^{2} \beta_j \boldsymbol{r}(\xi_i, \eta_j, \zeta), \qquad \boldsymbol{r}_\eta \boldsymbol{r}_\zeta = \sum_{j=1}^{2} \beta_j \sum_{k=1}^{2} \gamma_k \boldsymbol{r}(\xi, \eta_j, \zeta_k)$$

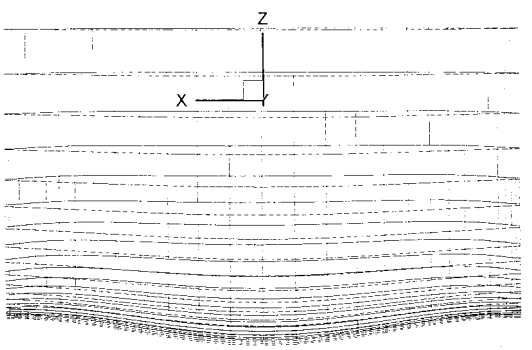

(a) case1

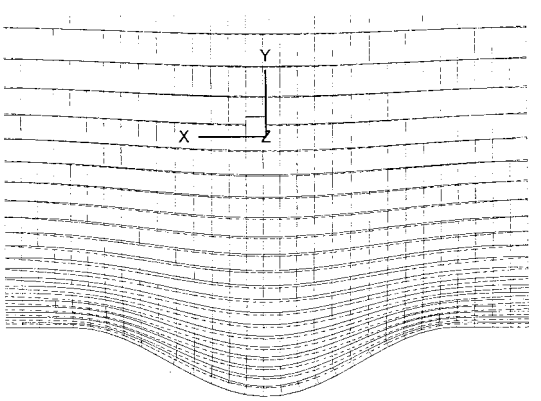

(b) case2

Figure 3. Comparison of the grids at $k = 25$ for case 1 and $k = 5$ for case 2 (solid, elliptic grid; dashed, algebraic grid).

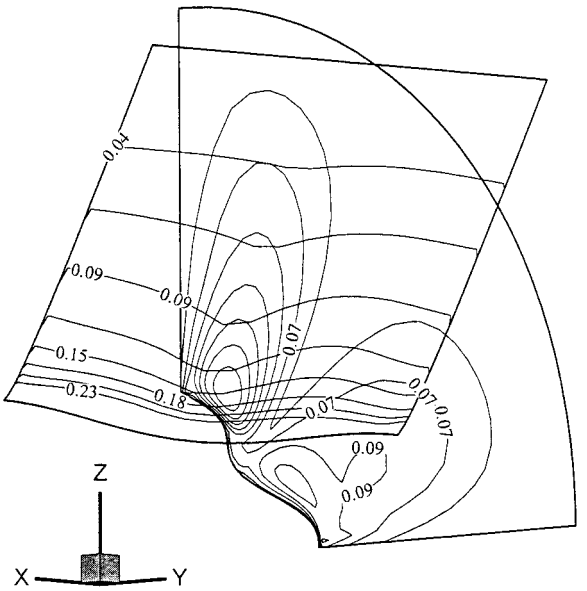

Figure 4. The orthogonality contours at $i = 15$, $i = 21$ for case 1.

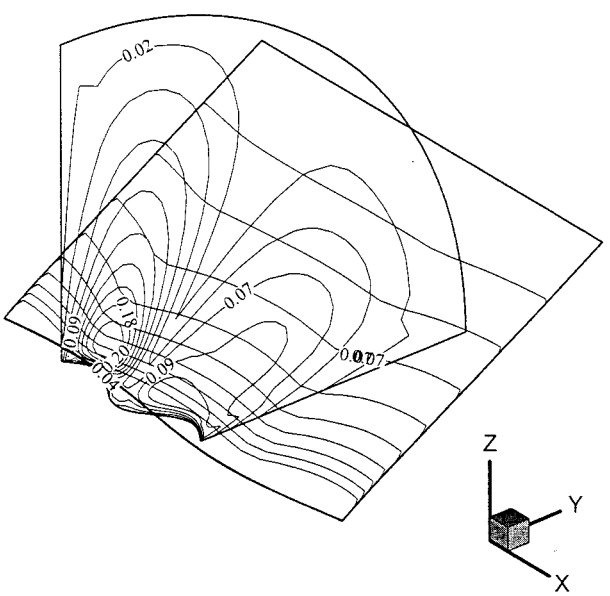

Figure 5. The orthogonality contours at $i = 15$, $k = 11$ for case 2.

$$\boldsymbol{r}_\zeta \boldsymbol{r}_\eta = \sum_{k=1}^{2} \gamma_k \sum_{i=1}^{2} \alpha_i \boldsymbol{r}(\xi_i, \eta, \zeta_k), \quad \boldsymbol{r}_\xi \boldsymbol{r}_\eta \boldsymbol{r}_\zeta = \sum_{i=1}^{2} \alpha_i \sum_{j=1}^{2} \beta_j \sum_{k=1}^{2} \gamma_k \boldsymbol{r}(\xi_i, \eta_j, \zeta_k)$$

where $\alpha_1 = \xi,\ \alpha_2 = 1 - \xi,\ \beta_1 = \eta,\ \beta_2 = 1 - \eta,\ \gamma_1 = \zeta,\ \gamma_2 = 1 - \zeta$. Two surfaces are arbitrarily constructed to have inflection points on the surfaces. The hyperbolic tangent function is used to generate the boundary grids.

3. APPLICATIONS AND RESULTS

Grid qualities are estimated in terms of concentration, smoothness and orthogonality, which are measured by the cell volume, arc length and intersection angles respectively. Eiseman [13] used the local interpolation functions for the multi-surface transformation, and Kerlick and Klopfer [14] reparameterized the Jacobian matrix and the metric tensor in two dimensions by analyzing the truncation error. The grid qualities are measured from the following concepts:

concentration:

$$(\boldsymbol{r}_\xi \cdot \boldsymbol{r}_\eta \times \boldsymbol{r}_\zeta)_{i,j,k}$$

smoothness:

$$\frac{1}{3} \sum_{m=i,j,k} \left(\frac{|\boldsymbol{r}_{m-1} - \boldsymbol{r}_0| + |\boldsymbol{r}_{m+1} - \boldsymbol{r}_0|}{|\boldsymbol{r}_{m-1} - \boldsymbol{r}_{m+1}|} - 1 \right) \quad \text{(fixing the other indices)}$$

orthogonality:

$$\frac{1}{8} \sum_{m=j\pm 1} \sum_{\substack{n=i\pm 1 \\ n=k\pm 1}} |(\boldsymbol{r}_m - \boldsymbol{r}_0) \cdot (\boldsymbol{r}_n - \boldsymbol{r}_0)| \quad \text{(fixing the other indices)}$$

where $\boldsymbol{r}_{m-1} = \boldsymbol{r}_{i-1,j,k}$ when $m = i$, $\boldsymbol{r}_m = \boldsymbol{r}_{i,j+1,k}$ when $m = j + 1$, and $\boldsymbol{r}_0 = \boldsymbol{r}_{i,j,k}$, etc. Since the concentration and smoothness can be handled in the algebraic grid, this analysis is focused on improving the grid orthogonality.

Figure 1 is the finally generated test grids and shows the surfaces inflection well. The grid sizes are $31 \times 21 \times 31$ (case 1) and $31 \times 31 \times 41$ (case 2). The boundary grids are moved to guarantee the orthogonality with keeping the original shape. This is confirmed in Figure 2. The careful consideration is required just near the highly curved surface because it is difficult to control simultaneously both the grid space and orthogonality. Especially, the grid lines on the lowest part in Figure 3(a) are moved a lot.

There are no significant changes in the concentrations and smoothness for both cases. However, the orthogonality is improved by 37 per cent (case 1) and 45 per cent (case 2). Figures 4 and 5 show the orthogonality contours in radians.

4. CONCLUSIONS

This paper shows three-dimensional elliptic grid generation assuming the main flow direction $x = x(\xi)$. A two-dimensional approach by modifying the Thomas–Middlecoff method is applied on the plane normal to x. The grid points on the boundaries are moved while maintaining orthogonality. Orthogonality is improved by about 40 per cent compared with those of the initial algebraic grid.

ACKNOWLEDGMENTS

This paper was funded by the Research Foundation of Engineering College, Sunchon National University.

REFERENCES

1. Eiseman PR. Grid generation for fluid mechanics computations. *Annual Reviews in Fluid Mechanics* 1985; **17**: 487–522.
2. Thompson JF, Weatherill NP. Numerical grid generation techniques. NASA CP 2166, 1990.
3. Thomas PD. Composite three-dimensional grids generated by elliptic systems. *AIAA Journal* 1982; **20**: 1195–1202.
4. Soni BK. Grid generation for internal flow configurations. *Computers and Mathematical Applications* 1992; **24**: 191–201.
5. Soni BK. Goodness of grid: quantitative measures. AIAA-88-3737, 1st National Fluid Dynamics Congress, Cincinnati, OH, July, 1988.
6. Soni BK, McClure MD, Mastine CW. Numerical grid generation in $N + 1$ easy steps. In *Proceedings of the Second International Conference of Numerical Grid Generation in Computational Fluid Dynamics*, Hauser J, Taylor C (eds). Pineridge Press: Landshut, Germany, 1986; 83–94.
7. Park S, Lee K. A Hypercube + + approach for multiblock structured grids. *Transactions of the KSME* 1997; **21**(7): 900–910.
8. Thompson JF, Warsi ZUA, Mastine CW. *Numerical Grid Generation*. North-Holland: Amsterdam, 1985.
9. Eiseman PR. A multi-surface method of coordinate generation. *Journal of Computers in Physics* 1979; **33**: 118–150.
10. Steger JL, Sorenson RL. Automatic mesh-point clustering near a boundary in grid generation with elliptic partial differential equations. *Journal of Computers in Physics* 1979; **33**: 405–416.
11. Kang S-H, Oh K-J, Kobayashi T. A viscous flow calculation of the stern flow. *KSME Journal* 1991; **5**(1): 36–44.
12. Middlecoff JF, Thomas PD. Direct control of the grid point distribution in meshes generated by elliptic equations. AIAA Paper 79-1462, 1979.
13. Eiseman PR. Coordinate generation with precise controls over mesh properties. *Journal of Computers in Physics* 1982; **47**: 331–351.
14. Kerlick GD, Klopfer GH. Assessing the quality of curvilinear coordinate meshes by decomposing the Jacobian matrix. In *Numerical Grid Generation*, Thompson JF (ed.). Elsevier: Amsterdam, 1982; 787–808.

